AD-A108 512 BATTELLE COLUMBUS LABS OH F/G 9/5
DESIGN OF A HIGHLY LINEAR CLOSED-LOOP FMCW SWEEP GENERATOR.(U)
AUG 79 P Z PEEBLES DAAG29-76-D-0100
UNCLASSIFIED DRSMI-RE-82-1-TR NL

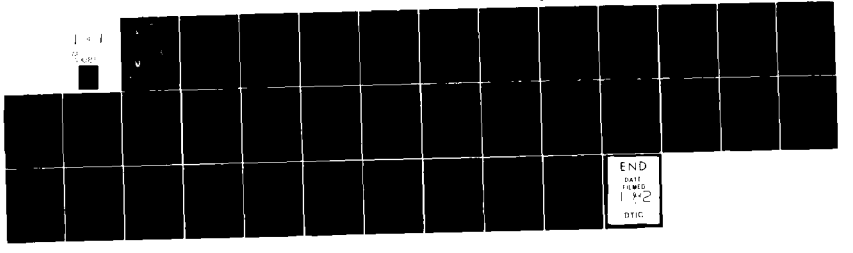

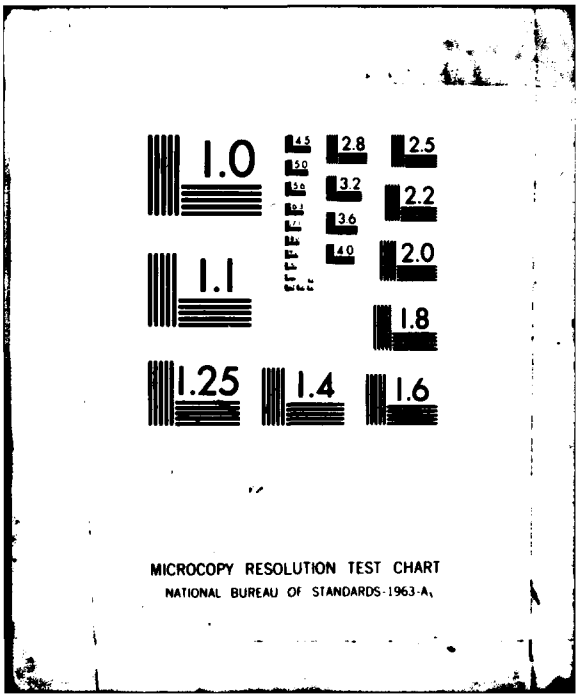
1.0
1.1
1.25
1.4
1.6
1.8
2.0
2.2
2.5
2.8
3.2
3.6
4.0
MICROCOPY RESOLUTION TEST CHART
NATIONAL BUREAU OF STANDARDS-1963-A

(12) LEVEL III

AD-E950181

TECHNICAL REPORT RE-82-1

ADA108512

DESIGN OF A HIGHLY LINEAR CLOSED-LOOP FMCW SWEEP GENERATOR

Peyton Z. Peebles, Jr.
University of Tennessee
Knoxville, Tennessee

8 August 1979

U.S. ARMY MISSILE COMMAND
Redstone Arsenal, Alabama 35809

Approved for public release; distribution unlimited.

DISPOSITION INSTRUCTIONS

DESTROY THIS REPORT WHEN IT IS NO LONGER NEEDED. DO NOT RETURN IT TO THE ORIGINATOR.

DISCLAIMER

THE FINDINGS IN THIS REPORT ARE NOT TO BE CONSTRUED AS AN OFFICIAL DEPARTMENT OF THE ARMY POSITION UNLESS SO DESIGNATED BY OTHER AUTHORIZED DOCUMENTS.

TRADE NAMES

USE OF TRADE NAMES OR MANUFACTURERS IN THIS REPORT DOES NOT CONSTITUTE AN OFFICIAL ENDORSEMENT OR APPROVAL OF THE USE OF SUCH COMMERCIAL HARDWARE OR SOFTWARE.

Unclassified

SECURITY CLASSIFICATION OF THIS PAGE *(When Data Entered)*

REPORT DOCUMENTATION PAGE

READ INSTRUCTIONS BEFORE COMPLETING FORM

1. REPORT NUMBER: Technical Report RE-82-1	2. GOVT ACCESSION NO.: D-A108 512
3. RECIPIENT'S CATALOG NUMBER	
4. TITLE *(and Subtitle)*: DESIGN OF A HIGHLY LINEAR CLOSED-LOOP FMCW SWEEP GENERATOR	5. TYPE OF REPORT & PERIOD COVERED
	6. PERFORMING ORG. REPORT NUMBER
7. AUTHOR(s): Peyton Z. Peebles, Jr. University of Tennessee Knoxville, Tennessee	8. CONTRACT OR GRANT NUMBER(s)
9. PERFORMING ORGANIZATION NAME AND ADDRESS Commander, US Army Missile Command ATTN: DRSMI-RE Redstone Arsenal, Alabama 35898	10. PROGRAM ELEMENT, PROJECT, TASK AREA & WORK UNIT NUMBERS
11. CONTROLLING OFFICE NAME AND ADDRESS Commander, US Army Missile Command ATTN: DRSMI-RPT Redstone Arsenal, AL 35898	12. REPORT DATE: 8 Aug 79 13. NUMBER OF PAGES: 33
14. MONITORING AGENCY NAME & ADDRESS*(if different from Controlling Office)*	15. SECURITY CLASS. *(of this report)*: Unclassified 15a. DECLASSIFICATION/DOWNGRADING SCHEDULE

16. DISTRIBUTION STATEMENT *(of this Report)*

Approved for public release; Distribution unlimited.

17. DISTRIBUTION STATEMENT *(of the abstract entered in Block 20, if different from Report)*

18. SUPPLEMENTARY NOTES

This report supersedes Technical Report RE-79-78, dated 8 August 1979.

19. KEY WORDS *(Continue on reverse side if necessary and identify by block number)*

Closed-loop linearizer
Voltage Controlled Oscillator (VCO)
Millimeter - Wave Transmitter
Butterworth filters
Frequency - Modulation
Instantaneous angular frequency
Mixer output angular frequency

20. ABSTRACT *(Continue on reverse side if necessary and identify by block number)*

This report describes results of work performed by the author for the RF Guidance Technology Branch of the Advanced Sensors Directorate, Technology Laboratory, US Army Missile Command, Redstone Arsenal, Alabama, during the summer of 1979, under a Scientific Services Agreement (D.O. 1172) with Battelle Columbus Laboratories authorized under contract DAAG29-76-D-0100. The technical representative for the US Army was Mr. Augustus H. Green, Jr.
(cont'd)

DD FORM 1 JAN 73 1473 EDITION OF 1 NOV 65 IS OBSOLETE

Unclassified

SECURITY CLASSIFICATION OF THIS PAGE *(When Data Entered)*

The basic task was to design and analyze a closed-loop method for linearizing the "linear" frequency-modulated (FM) transmission from a millimeter-wave transmitter at 35 GHz. The basic design was then to be constructed and evaluated as far as possible within existing time and equipment availability constraints.

ACKNOWLEDGEMENTS

The author expresses his appreciation to Messrs. C.H. Cash and A.H. Green, Jr., for their personal support, guidance and encouragement while working with the RF Guidance Technology Area during the Summer of 1979. He is especially grateful to Mr. Green for his guidance and helpful discussions during the work.

CONTENTS

ILLUSTRATIONS

Figure Page

1. INTRODUCTION.

A number of systems utilize transmitters that generate wave-forms that sweep in frequency from an initial value to a final value in a "linear" manner during some time period (T) and then repeat the transmission periodically. Some radio altimeters and missile radars during terminal guidance are examples of such systems where ultimate performance is related to how linear the "linear" sweep really is.

Most of the simple, direct ways of generating these linear frequency-modulation (FM) continuous wave (CW) sweeps produce linearities of only about ±(5-10)% (one hundred times the ratio of maximum frequency deviation from the ideal linear function during T, divided by the desired frequency change (B) during T, is defined as percentage linearity). In many applications such linearity is grossly unacceptable so some form of linearizer is usually employed.

Linearization methods basically fall into two categories: open-loop, and closed-loop. Open-loop methods can produce linearities on the order of perhaps ±0.1% at best, while closed-loop systems can yield linearity on the order of ±0.002% [1].†

This report describes the design and evaluation of a closed-loop linearizer which appears to be the most promising approach at the present time. The design is applicable to a transmitter at 35 GHz that generates a linear sweep of 1 GHz.

2. THE CLOSED-LOOP LINEARIZER.

Several different forms of closed-loop sweep linearizers are possible. The various systems have been described in an earlier report [1] and are not compared in detail here. We only state that the closed-loop system that seems the most promising from the standpoints of simplicity and performance is the implementation shown in *Figure 1*.

A. THE BASIC LOOP.

In describing the operation of the loop of *Figure 1* let it first be assumed that the voltage-controlled oscillator (VCO) is ideal. That is, it has a perfectly linear frequency-versus-voltage characteristic. For an ideally linear sweep command voltage the ideal VCO output frequency would behave with time as shown in *Figure 2* (solid curve). The output of the delay line in

† References listed at the end of this report are quoted by bracketed number.

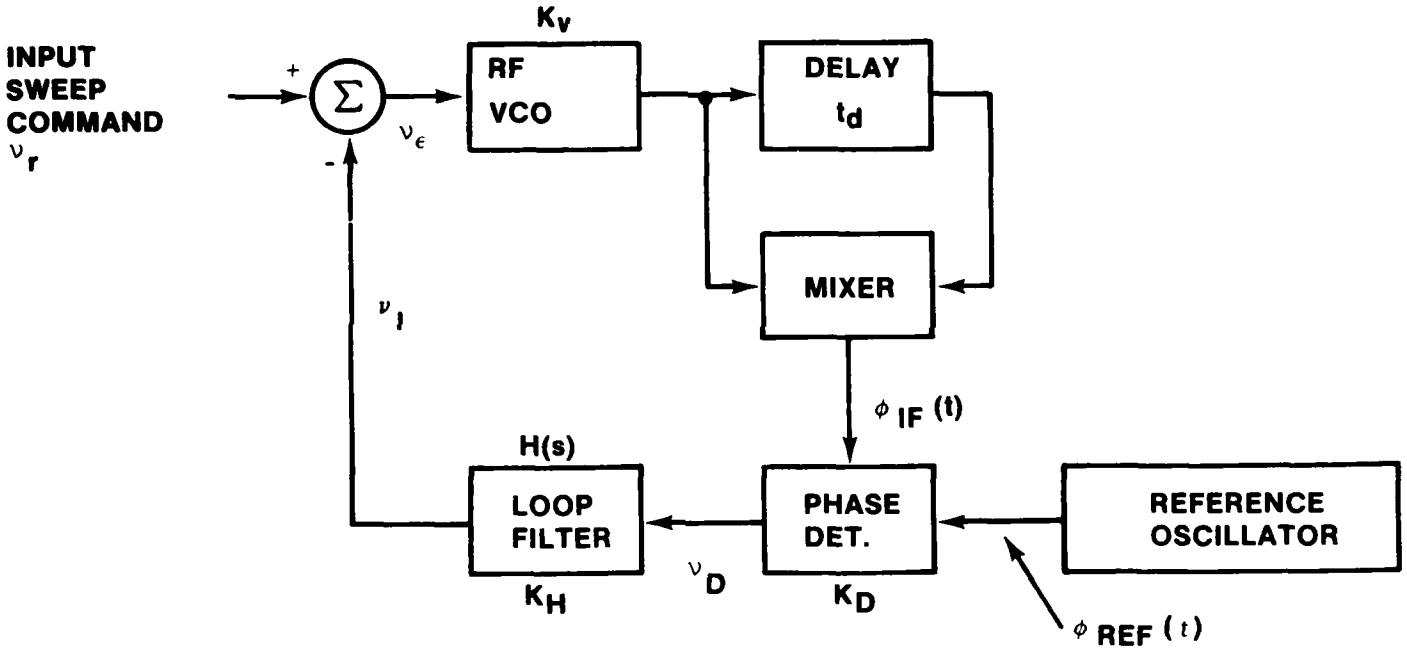

Figure 1. The basic closed-loop sweep linearizer.

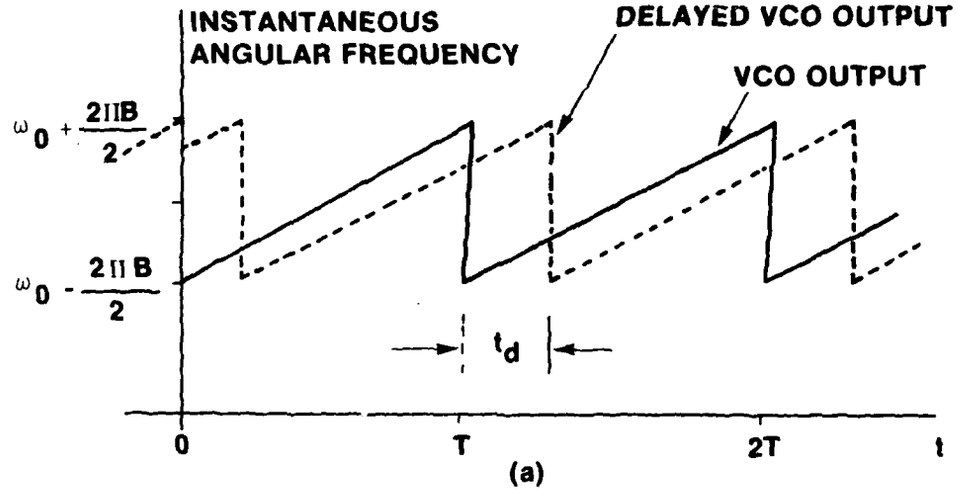

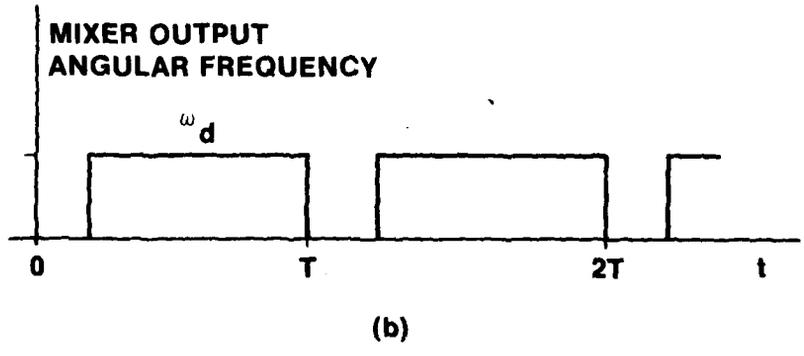

Figure 2. Frequency plots.

Figure 1 will have an instantaneous frequency versus time as shown dashed in *Figure 2*(a). The mixer produces a signal with a frequency that is the difference of the frequencies of its two inputs. In practical systems t_d is a small delay relative to T so the output frequency of the mixer is as shown in *Figure 2*(*b*) where $\omega_d = 2\pi B t_d / T$ with B(Hz) being the frequency sweep that occurs in time period T (seconds).† By choosing the angular frequency of the reference oscillator equal to ω_d the output of the phase detector can be made zero. As discussed later, there is a nonzero output due to unequal phases of the two phase detector inputs, but this output only represents a quickly corrected transient term in the loop. Thus, when the VCO generates an ideal linear frequency sweep the loop feedback signal is zero.

In all practical systems the VCO is not ideal. We can represent the nonideal sweep by an ideal sweep plus an error component. Let $\omega_1(t)$ represent the departure of the actual sweep instantaneous angular frequency from the ideal linear value. Later analysis will show that the loop now generates an error voltage v_1 proportional to $\omega_1(t)$ that can be used to reduce $\omega_1(t)$ and improve linearity by closed-loop methods.

B. THE PRACTICAL LOOP.

It results that performance of the linearizer of *Figure 1* improves as both closed-loop bandwidth and t_d increase. However, increasing t_d can ultimately limit the useable bandwidth. Since many systems are ultimately designed to achieve a certain closed-loop bandwidth, it becomes necessary to select t_d as large as possible consistent with its bandwidth constraint. For example, if β_L (rad/s) is the desired closed-loop linearizer bandwidth, it can be shown that

$$t_d \lesssim \pi/2 \; \beta_L \tag{1}$$

is necessary for good loop performance. However, selection of t_d to satisfy Equation (1) can lead to a practical problem in broadband systems.

Suppose $\beta_L / 2\pi = 10^7$ Hz is desired. Then, from Equation (1), $t_d \lesssim 25$ns, which is reasonable. However, note that this value of t_d corresponds to a difference frequency out of the mixer in *Figure 1* of

† The mixer output frequency is actually large during time intervals $nT < t \leq nT + t_d$, $n = 0, \pm 1, \pm 2 \cdots$. However, these components are short in duration and are not important to the performance of the closed-loop. We assume they have been removed in drawing *Figure 2* (*b*).

$$f_d = Bt_d/T = 2.5 \text{ MHz} . \quad (2)$$

if we assume B=1.0GHz and T=10μs. This value of f_d is less than the loop bandwidth and direct leakage through a practical phase detector can reduce performance. To prevent the leakage, a frequency offset f_i can be added to f_d by using the circuit of *Figure 3*

Practical considerations of *Figure 3* for large bandwidth RF sweeps (order of B=1GHz) show that f_1 needs to be at least several times B so that direct leakage through mixer 1 does not show up at mixer 2. Larger values of f_1 create other problems. First, the phase detector must now operate at very high frequency, opening up the possibility of phase stability problems. Second, the delay becomes harder to realize at lower RF frequencies because, as f_1 increases, B becomes a larger fraction of allowable standard waveguide bandwidth. Finally, unless f_i is quite large relative to B, the filtering of undesired mixer 1 products is difficult. These problems can all be relieved by using the circuit of *Figure 4*.

By using an offsetting mixer in each of the channels feeding mixer 3 the difference frequency $(f_1-f_2)+f_d$ can be set to a convenient value, the delay line center frequency can be chosen at will (to a value where nondispersive coaxial line delay can be used for example), and both f_0-f_1 and f_0-f_2 can be selected so that mixing products of mixers 1 and 2 can readily be filtered. The system selected for construction in this study was that of *Figure 4*.

3. PRACTICAL LOOP DESIGN.

The practical design of the system of *Figure 4* amounts to selecting a closed-loop bandwidth, selecting frequencies f_1 and f_2, and choosing a delay time t_d. It is assumed that specified system parameters are:

B=1.0 GHz

T=(10-100) μs variable

f_0=35.0 GHz.

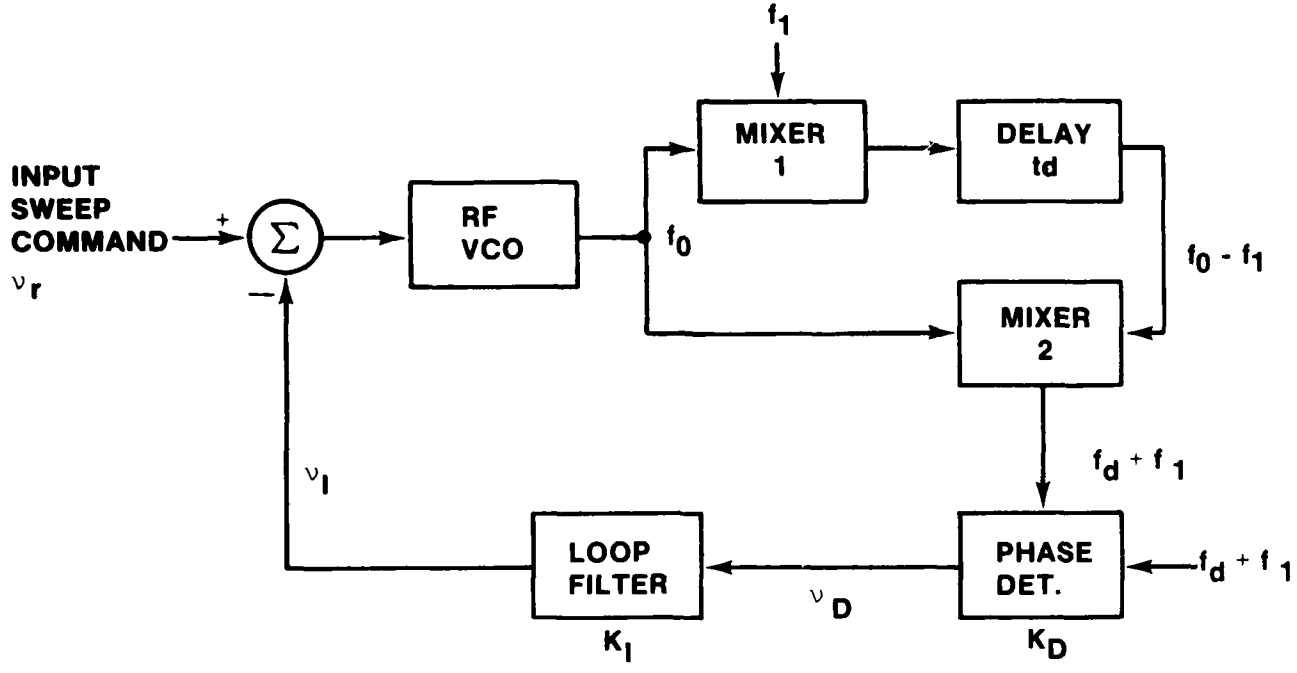

Figure 3. Modified closed-loop sweep linearizer using one offsetting local oscillator.

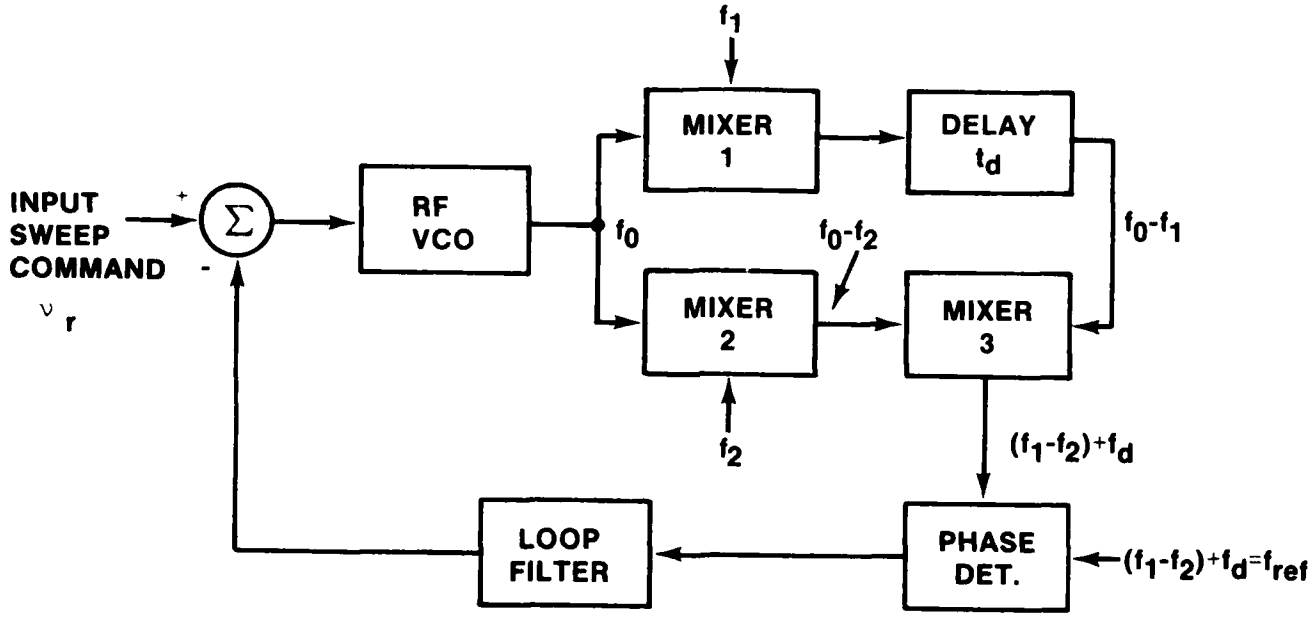

Figure 4. Modified closed-loop sweep linearizer using two offsetting local oscillators.

A. BANDWIDTH SELECTION.

One of the most severe errors for which the loop must correct is a slight error in slope of the RF sweep. The frequency error to be corrected therefore appears as shown in *Figure 5*. We arbitrarily select loop bandwidth β_1 2π equal to the frequency above which all components of frequency in the function of *Figure 5* have a total of less than 0.6% of the power of all harmonic components.

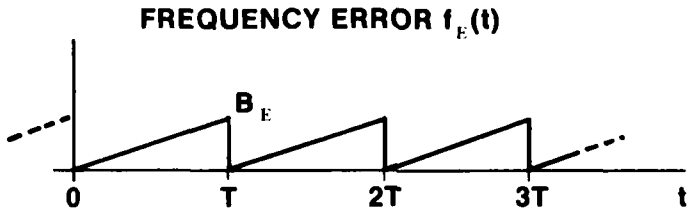

Figure 5. Frequency error.

By expanding $f_1(t)$ into its Fourier series to find the Fourier series coefficients, and using these in the power spectrum $S_1(\omega)$ of $f_1(t)$, we obtain: [4, p. 43]

$$S_E(\omega) = 2\pi \left\{ \frac{B_E^2}{4} \delta(\omega) + \frac{B_E^2}{4\pi^2} \sum_{n=1}^{\infty} \frac{1}{n^2} \left[\delta(\omega - n\omega_T) + \delta(\omega + n\omega_T) \right] \right. \quad (3)$$

where

$$\omega_T = 2\pi/T . \quad (4)$$

The total power in the frequency interval $-N\omega_1 \leq \omega \leq N\omega_1$, where $N \geq 1$ is an integer, is found by integration

$$P_{N\omega_T} = \frac{1}{2\pi} \int_{-N\omega_T}^{N\omega_T} S_E(\omega)\, d\omega$$

$$= \frac{B_E^2}{12} \left[3 + \frac{6}{\pi^2} \sum_{n=1}^{N} (1/n^2) \right] . \quad (5)$$

The term $B_1^2/4$ is the dc power which is of minor importance (represents a small fixed frequency error for the loop to correct). The second term represents ac power. It is known [5, p. 44-6] that

$$\sum_{n=1}^{\infty} \frac{1}{n^2} = \frac{\pi^2}{6}, \tag{6}$$

so $B_1^2/12$ is the total ac power, P_{ac}, in $f_1(t)$. From Equation (5) the fractional amount of ac power outside the band $-N\omega_1 \leq \omega \leq N\omega_1$ becomes

$$\left.\begin{array}{l}\text{Fractional ac}\\ \text{power outside}\\ -N\omega_1 \leq \omega \leq N\omega_1\end{array}\right\} \triangleq F = 1 - \frac{6}{\pi^2} \sum_{n=1}^{N} \left(\frac{1}{n}\right)^2. \tag{7}$$

The sum is related to the polygamma function $\psi'(\cdot)$ of order one which is [6, p. 260].

$$\psi'(N+1) = \frac{\pi^2}{6} - \sum_{n=1}^{N} \left(\frac{1}{n}\right)^2. \tag{8}$$

Thus,

$$F = \frac{6}{\pi^2} \psi'(N+1) \simeq \frac{6}{\pi^2 (N+1)}, \quad N >> 1, \tag{9}$$

where $\psi'(N+1) \approx 1/(N+1)$ for $N >> 1$ [6, p. 260]. For a fractional ac power $F \leq 0.006$ (0.6%) we require $N \geq 100$ from Equation (9). Loop bandwidth becomes

$$\beta_L / 2\pi = N/T = 100/\left[10^{-5}\right] = 10\text{MHz} \tag{10}$$

for $T = 10\mu s$ (worst case).

B. SELECTION OF f_1 AND f_2.

Assume $(f_1-f_2) >> f_d$. The difference between f_1 and f_2 can first be found by considering the phase detector in *Figure 4*. If a filter is to remove the direct leakage at frequency $(f_1-f_2)-(\beta_L/2\pi)$ then, assuming low pass filter bandwidth of $3\beta_L/2\pi$ (several times $\beta_L/2\pi$,) we require

$$\frac{(f_1-f_2) - (\beta_L/2\pi)}{3\beta_L/2\pi} > M \text{ or } (f_1-f_2) \geq \beta_L (3M+1)/2\pi \tag{11}$$

where M is a constant related to the number of poles in the filter. For a Butterworth filter attenuation is related to M in *Figure 6*. It is actually the ratio of the lowest frequency we wish to eliminate, which is $(f_1-f_2)-(\beta_1 \ 2\pi)$, to the band width $3\beta_1 \ 2\pi$ of the low-pass filter.

In a phase detector (Hewlett-Packard 10514A, for example) leakage can be about 6dB below the output signal. If over -80dB is an acceptable leakage level and the loop filter is assumed to give as much attenuation as the low-pass filter (it typically will give more) and is assumed to have at least two poles, then we require M≈8.5 from *Figure 6*. Thus,

$$(f_1-f_2) \gtrsim 10^7 \ (25.5 + 1) = 265 \ \text{MHz}. \tag{12}$$

A value (f_1-f_2) = 300 MHz was chosen.

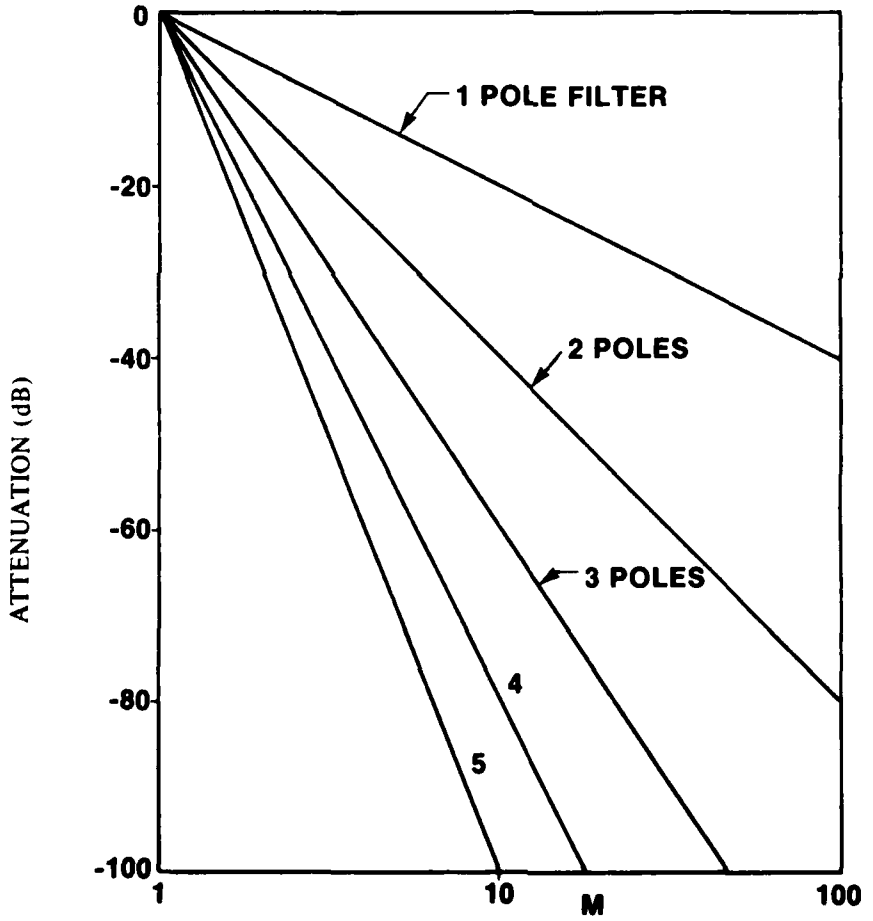

Figure 6. Attenuation of Butterworth filters.

Leakages through mixer 3 are not expected to affect loop performance appreciably. However, f_1 can be selected to allow for filtration, if needed. If the lowest frequency of the leakage, which is $f_0-f_1-(B/2)$, is to be attenuated over 60dB by a three-pole band-pass filter at 300MHz with a half-bandwidth of 60MHz then $f_1 \leq 33.6$GHz. A value of $f_1=33.5$ GHz was selected in the system. Since $f_1-f_2=0.3$ GHz, then $f_2=33.2$ GHz.

C. SELECTION OF DELAY TIME.

For good loop performance Equation (1) must be satisfied so $t_d \leq 1/[4(10^7)]=25$ ns. Ordinarily $t_d=25$ns would be selected. However, in the present system T is variable and practical considerations lead to another value.

To make the system independent of variations in T we note that

$$f_d = Bt_d/T \quad . \tag{13}$$

Now if t_d (which varies in the system because T varies) is made a multiple N of 1/T, then

$$f_d = N/T \quad . \tag{14}$$

On equating Equation (13) and Equation (14) we have

$$t_d = N/B = N \text{ ns.} \tag{15}$$

From practical considerations N=16 is the largest binary value of N for which $t_d \leq 25$ns.

D. SYSTEM BLOCK DIAGRAM.

Figure 7 is the block diagram of a system having the characteristics described above. Part of the block diagram is a local oscillator generator that generates the necessary frequencies $f_1=33.5$ GHz, $f_2=33.2$ GHz, $f_{LO}=300$ MHz + 16 f_R, $f_R = 1/T$, T=(10-100)μs.

4. LOOP PERFORMANCE.

In this section the performance of the closed loop system of *Figure 7* is discussed. Only the most important performance measures are considered. First, the affects of phase instabilities in the local oscillator generator are developed followed by a detailed developments of a

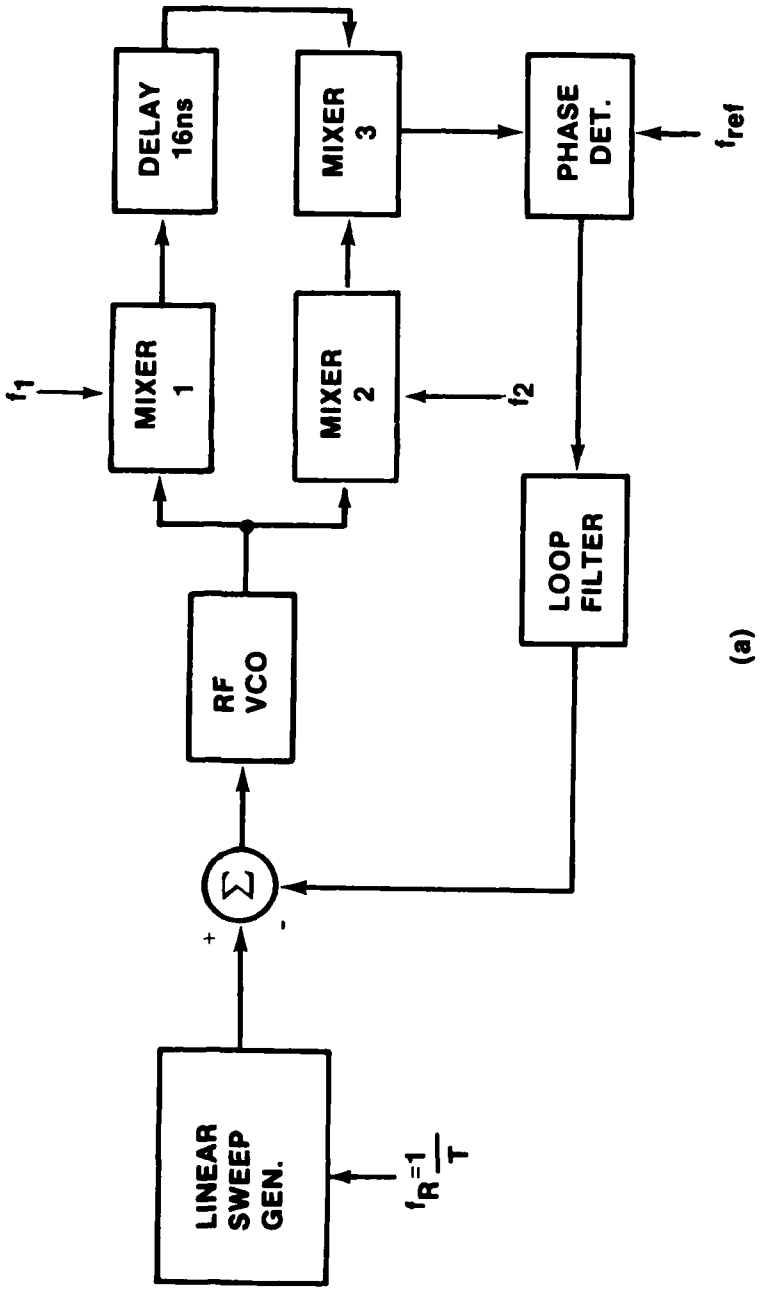

Figure 7. System block diagram.

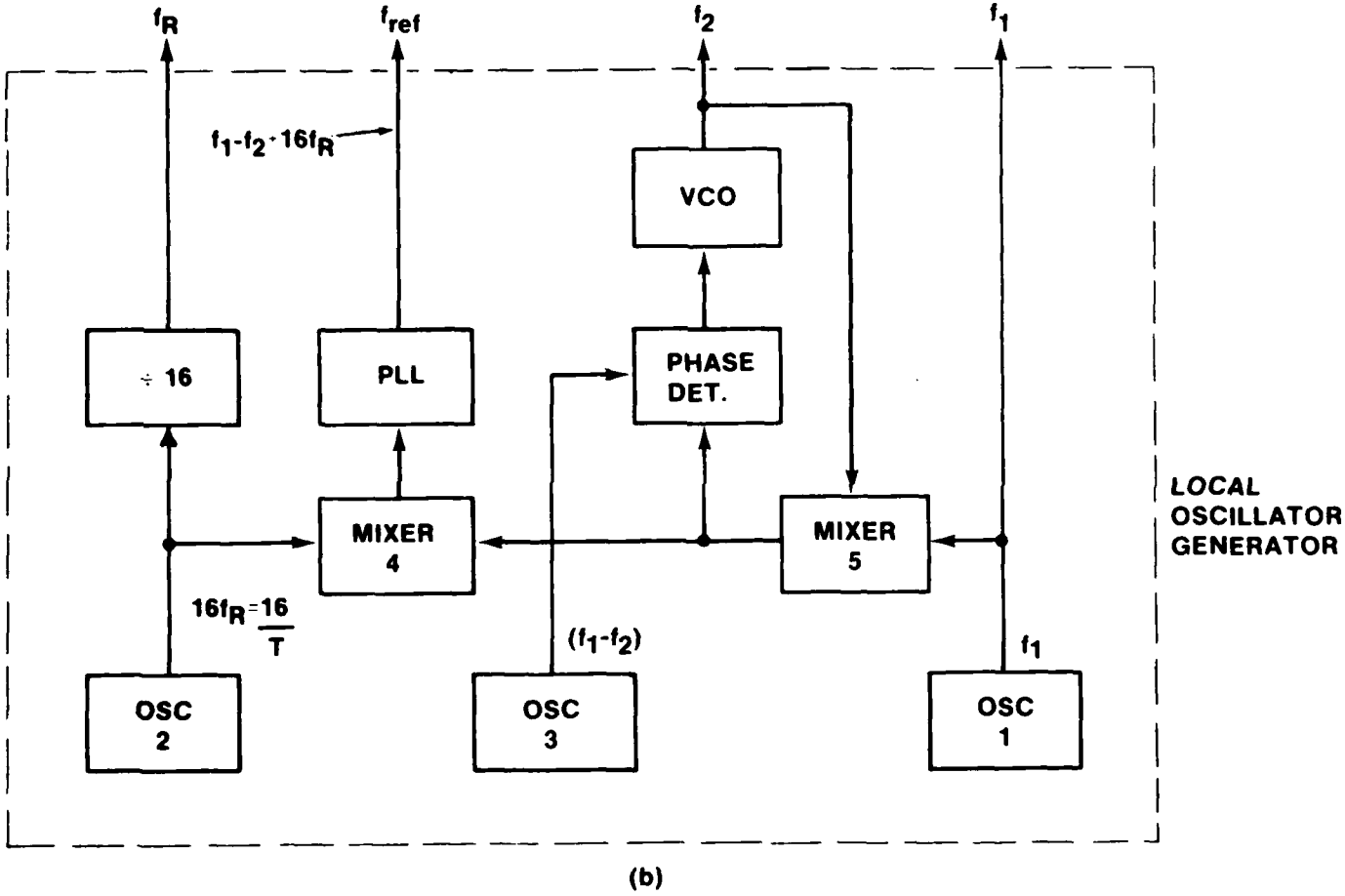

(b)

Figure 7. (Concluded)

linearized model for the loop. Finally, the transient and error linearization performance are developed.

A. LOCAL OSCILLATOR GENERATOR INSTABILITIES.

Consider the affects of slowly varying phase instabilities $\delta\phi_1$, $\delta\phi_2$, and $\delta\phi_{ref}$ that occur, respectively, on the outputs in *Figure 7 (b)* that have frequencies f_1, f_2, and f_{ref}. By slowly varying we mean the instabilities may be taken as approximately constant during any interval of duration T. Instability $\delta\phi_1$ enters directly into the main loop of (a) and results in the phase $\delta\phi_1$ at the phase detector input.

Next, consider finding $\delta\phi_2$. At the output of mixer 5 in *Figure 7 (b)* the instability is $\delta\phi_1$-$\delta\phi_2$. If $\delta\phi_3$ denotes the phase instability of oscillator 3, the phase detector produces a voltage proportional to the VCO loop phase error, denoted by δE_2, given by $\delta E_2=\delta\phi_1-\delta\phi_2-\delta\phi_3$. Thus,

$$\delta\phi_2 = \delta\phi_1 - \delta\phi_3 - \delta E_2 \quad . \tag{16}$$

By use of Equation (16) the phase instability at the output of mixer 5 becomes $\delta\phi_3+\delta E_2$. This same instability is applied to the phase-locked loop (PLL) that generates frequency f_{ref} having phase instability $\delta\phi_{ref}$. If δE_1 denotes the amount that $\delta\phi_{ref}$ differs from its input command $\delta\phi_3+\delta E_2$ then

$$\delta\phi_{ref} = \delta\phi_3 + \delta E_2 + \delta E_1 \quad . \tag{17}$$

In *Figure 7(a)* the instability $\delta\phi_2$ of Equation (16) propagates to the input of the phase detector as $-\delta\phi_2= -\delta\phi_1+\delta\phi_3+\delta E_2$. The total phase instability at the phase detector input becomes $\delta\phi_1-\delta\phi_2=\delta\phi_3+\delta E_2$. The loop phase detector generates a voltage proportional to the difference in phase between its two inputs. Its difference phase due to local oscillator instabilities becomes $(\delta\phi_3+\delta E_2)-\delta\phi_{ref}= -\delta E_1$ when Equation (17) is used.

From the foregoing discussion it is clear that all phase instabilities of the local oscillator generator in *Figure 7 (b)* cancel in the main loop except that of the PLL tracking error. It is therefore important that the PLL static error be small through design. These conclusions neglect any errors in oscillator 2. Consider its affect next.

Suppose in a given sweep interval f_R is slightly different than desired by an amount δf_R. From Equation (13) the change in the difference frequency f_d at the input to the loop phase

detector is $\delta f_d = B t_d \delta f_R$. But from Equation (15) $\delta f_d = N \delta f_R$ where N=16. Since the frequency change on f_{ref} of *Figure 7* is similarly $\delta f_{ref} = N \delta f_R = 16 \delta f_R$ there is no net error at the loop phase detector output. This evaluation only verifies that our previous selection of delay t_d to make the system independent of the actual value of f_R was correct.

B. LINEARIZED LOOP MODEL.

From the standpoint of anaylizing the transient and static behavior of the system of *Figure 7* the frequency shifting circuitry can be neglected and analysis can center on the system of *Figure 1*. Define K_V (rad/s per volt) as the desired "gain" of the VCO, K_D (V/rad) as the "gain" of the phase detector and K_H (V/V) as the dc gain of the loop filter that has a voltage transfer function H(s).

Consider the system first in an open-loop condition obtained by opening the line at the loop filter's output. Ideally the VCO should produce a frequency sweep of B(Hz) in a time interval T(s). The required sweep command therefore is

$$v_r(t) = \frac{B}{K_V T} \quad t \ , \ 0 \leq t \leq T \ . \tag{18}$$

Such a command would ideally generate a VCO output angular frequency of $\omega_i + (2\pi B/T)t$, $0 \leq t \leq T$ where ω_i is the initial angular frequency at t=0. However, the VCO is not perfectly linear and an error term occurs that we denote by $\omega_E(t)$. The actual VCO angular frequency becomes $\omega_{VCO}(t) = \omega_i + (2\pi B/T)t + \omega_E(t)$. Since phase is the time integral of angular frequency, the phase of the actual VCO output, denoted $\phi_{VCO}(t)$, is

$$\phi_{VCO}(t) = \int_{-\infty}^{t} \omega_{VCO}(\xi)\, d\xi \tag{19}$$

$$= \omega_i t + (\pi B/T)\, t^2 + \theta_V + \int_{-\infty}^{t} \omega_E(\xi)\, d\xi$$

where θ_V is a phase constant of integration representing the phase of the VCO at time t=0.

At the loop mixer the phase of one input is given by (19) while the other is $\omega_i(t-t_d) + (\pi B/T)(t-t_d)^2 + \theta_V + \int_{-\infty}^{t-t_d} \omega_E(\xi)\, d\xi$.

Thus
$$\phi_{IF}(t) = \left[\omega_i t_d - (\pi B/T)\ t_d^2\right] + (2\pi B\ t_d/T)\ t + \int_{t-t_d}^{t} \omega_E(\xi)\ d\xi \quad , \tag{20}$$

which is the difference in input phases. The quantity $(2\pi B t_d/T)$ is the difference angular frequency ω_d caused by the delay t_d. It is the angular frequency of the reference signal. Let

$$\phi_{ref}(t) = \omega_d t + \theta_{ref} \tag{21}$$

be the phase of the reference signal where θ_{ref} is a constant. The phase detector output will be proportional to the sine of the difference phase $\phi_{ref}(t) - \phi_{IF}(t)$, in general. However, if the difference phase is small, which amounts to linearizing the loop, then

$$\nu_D(t) = K_D \left\{\left[\theta_{ref} - \omega_i t_d + (\pi B t_d^2/T)\right] - \int_{t-t_d}^{t} \omega_E(\xi)\ d\xi \right\} . \tag{22}$$

Now even though θ_{ref} can be made the same from sweep-to-sweep [*See Equation (14)*] there is no control of ω_i and T can change from sweep-to-sweep.

Therefore

$$\theta_E = \theta_{ref} - \omega_i t_d + (\pi B t_d^2/T) \tag{23}$$

represents a constant (in one sweep period) phase error that the loop must null out on every sweep.

In general, θ_E may initially be large enough so that the linearized Equation (22) does not hold. However, once the loop has nulled the large error, it is reasonable to expect that over a number of sweeps ω_i and $1/T$ will not change so rapidly that Equation (22) will not hold. We shall therefore assume in the following work that θ_E is a small phase error.

It is to be noted that Equation (22) results even if the ideal linear sweep of the VCO is removed. In other words, with respect to loop correction of errors $\omega_E(t)$, we can let ν_r in *Figure 1* be zero. With this and earlier considerations in mind, the equivalent loop of *Figure 8* can be

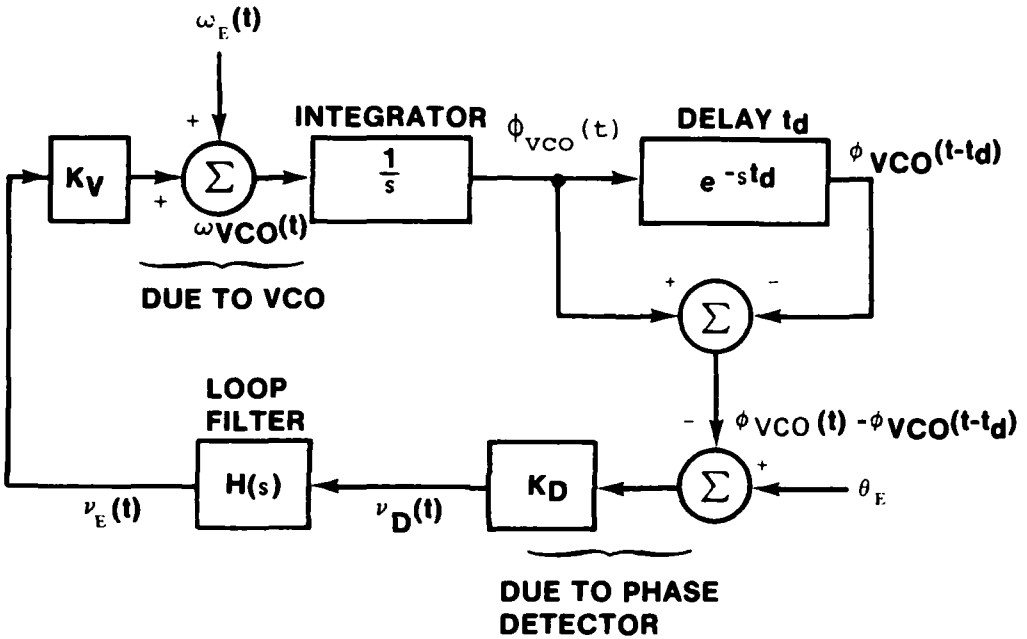

Figure 8. Linearized loop block diagram.

used to analyze transient performance in correcting for error $\omega_I(t)$. The transfer functions of the blocks are shown in s-domain notation. Because only errors are now involved, $\omega_{VCO}(t)$ represents the residual or uncorrected nonlinearity in the VCO angular frequency.

If $\omega_{VCO}(s)$, $\omega_I(s)$ and $\theta_I(s)$ are the Laplace transforms of $\omega_{VCO}(t)$, $\omega_I(t)$ and $\theta_I(t)$, respectively, it is found that

$$\omega_{vco}(s) = \frac{\omega_E(s) + K_v K_D H(s)\ \theta_E(s)}{1+K_v K_D H(s) e^{-st_d/2}\left[\dfrac{e^{st_d/2} - e^{-st_d/2}}{s}\right]} .$$

To simplify Equation (24) let $s=j\omega$ and note that

$$e^{-j\omega t_d/2}\left[\frac{e^{j\omega t_d/2} - e^{-j\omega t_d/2}}{j\omega}\right] = t_d \frac{\sin(\omega t_d/2)}{(\omega t_d/2)} e^{-j\omega t_d/2}$$

$$\simeq t_d \quad \text{if} \quad \omega << 2\pi/t_d . \qquad (25)$$

This condition is met in all practical systems so

$$\boxed{\omega_{vco}(s) = \frac{\omega_E(s) + K_v K_D\ H(s)\ \theta_E(s)}{1 + K_v K_D t_d\ H(s)}} . \qquad (26)$$

becomes the basic equation for use in modeling transient behavior.

C. TYPES OF LOOPS.

Choice of loop filter determines the type of loop. For example if $H(s)=K_H$ (a constant) the loop is said to be type 0. Based on stability considerations surrounding the approximation [Equation (25)] it can be found that loop gain $K=K_v K_D t_d K_H$ is limited to about 3.2 (10dB). This fact makes the type 0 loop impractical for present purposes.

If the loop transfer function has the form

$$H(s) = \frac{K_H}{1 + \tau_0 s} , \qquad (27)$$

where K_H and τ_0 are constants, the loop is approximately type I if $|\tau_0 s| >> 1$ for most frequencies of interest. In other words, $H(s) \approx K_H \tau_0 s$, an integrator. This form of loop is stable and capable of higher loop gains than is type 0 but not as high as a type II loop, for the same bandwidth.

An approximately type II loop results when H(s) has the form

$$H(s) = \frac{K_H (1 + \tau_2 s)}{(1 + \tau_0 s)(1 + \tau_1 s)} , \tag{28}$$

where $\tau_0 > \tau_1 > \tau_2$ are constants. This form of filter has been assumed in following work. It provides high loop gain with good stability if properly compensated (choice of τ_1 and τ_2).

D. TRANSIENT PERFORMANCE.

By substitution of Equation (28) in Equation (26) and considering only the term involving frequency error $\omega_I(s)$ we have

$$\omega_{VCO}(s) = \frac{\omega_E(s) \left[1+(\tau_0+\tau_1)\, s + \tau_0\tau_1\, s^2\right]}{(1+K) + (\tau_0+\tau_1+K\tau_2)s+\tau_0\tau_1 s^2} \tag{29}$$

where

$$K = K_V K_D K_H t_d \cdot \tag{30}$$

Now the transient behavior of the corrected error [inverse Laplace transform of Equation (29)] depends on the choice of loop parameters K, τ_0, τ_1, and τ_2. If β_0 is defined as the angular frequency where the open-loop gain of the system is unity (0dB), then a reasonable and somewhat conservative (with respect to gain and phase margins) design is defined in *Figure 9* where

$$K = 1000\sqrt{10} \tag{31}$$

$$\tau_0 = 100\sqrt{10}/\beta_0 \tag{32}$$

$$\tau_1 = 100/\beta_0 \tag{33}$$

$$\tau_2 = 10/\beta_0 \tag{34}$$

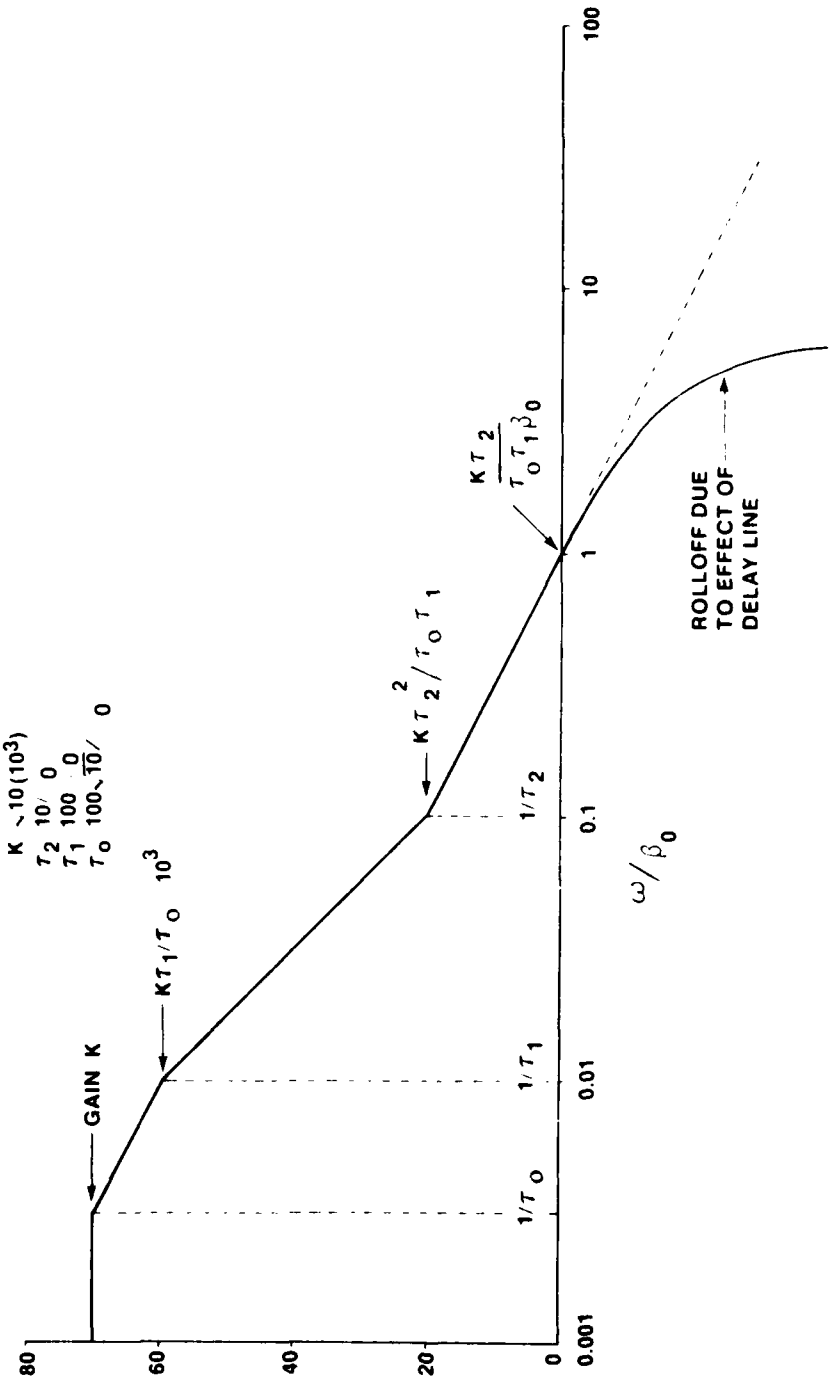

Figure 9. Open-loop gain.

and $\beta_0 = 2\pi(10^3)$ rad/s in the system. With these parameters Equation (29) has the form

$$\omega_{vco}(s) = \frac{\omega_E(s)\left[a_0 + a_1 s + s^2\right]}{(s+\alpha)(s+\gamma)} \tag{35}$$

where

$$a_0 = \frac{1}{\tau_0\tau_1} = 10^{-5}\sqrt{10}\,\beta_0^2 \simeq 3.1623(10^{-5})\,\beta_0 \tag{36}$$

$$a_1 = (\tau_0+\tau_1)/\tau_0\tau_1 = 10^{-3}\,(10+\sqrt{10})\,\beta_0 \simeq 0.01316\,\beta_0 \tag{37}$$

$$\alpha = \frac{\tau_0 + \tau_1 + K\tau_2}{2\tau_0\tau_1}\left\{1 + \sqrt{1 - \frac{4(1+K)\,\tau_0\tau_1}{(\tau_0+\tau_1+K\tau_2)^2}}\right\}$$

$$\simeq 0.9023\,\beta_0 \tag{38}$$

$$\gamma = \frac{\tau_0 + \tau_1 + K\tau_2}{2\tau_0\tau_1}\left\{1 - \sqrt{1 - \frac{4(1+K)\,\tau_0\tau_1}{(\tau_0+\tau_1+K\tau_2)^2}}\right\}$$

$$\simeq 0.1109\,\beta_0 \quad . \tag{39}$$

- Step of Error

If a step $\Delta\omega$ of frequency error is to be corrected by the loop, then $\omega_i(s) = \Delta\omega/s$ and

$$\frac{\omega_{vco}(s)}{\Delta\omega} = \frac{a_0 + a_1 s + s^2}{s(s+\alpha)(s+\gamma)} \quad . \tag{40}$$

The inverse Laplace transform of Equation (40) is known. After substitution of Equations (36) through (39) we have

$$\frac{\omega_{vco}(t)}{\Delta\omega} \simeq 3.16(10^{-4}) + 1.12\,e^{-0.9\beta_0 t}$$

$$- 0.124\,e^{-0.11\beta_0 t}\,, \quad t>0 \quad . \tag{41}$$

For practical values of $\Delta\omega$ the constant term is negligible. The first transient term in Equation (41) quickly dies out and equals the second term at $t = 2.79\ \beta_0$. Thereafter the second term dominates.

A step is important in the system because the VCO may not return to the same initial frequency from sweep-to-sweep due to VCO instability and to errors in the initial sweep voltage on the VCO. Suppose the VCO ramps 1000 MHz with 25V of sweep. Then an initial sweep voltage error of only 1% can cause 10 MHz of initial frequency error. From Equation (41) it will take approximately $t = 23\ \beta_0 = 0.37\mu s$ for the error to be reduced to 0.01% of the sweep of 1000 MHz. In the case where $T = 10\mu s$ this is transient or recovery interval is 3.7% of the sweep period. Because of these facts, tight control of the initial sweep frequency may be necessary.

It should be noted that a fixed frequency error in the sweep shows up in the loop as a constant phase error $\Delta\omega t_d$ arising from the term $K_p\omega_i t_d$ in Equation (23). Thus, the above consideration of a step of error has actually done the equivalent of evaluating the phase error term θ_1 of Equation (23). To see this fact, observe that θ_1 in *Figure 8* can be moved up to the summing point with $\omega_i(t)$ by allowing another (constant) frequency error of θ_1 / t_d (rad/s). For the above $\Delta\omega = 2\pi$ of 10 MHz we have $\theta_1 = 2\pi(10^7)t_d = 0.32\ \pi$ rad or 57.6 degrees of phase error. Thus, ±10 MHz of initial sweep frequency error is equivalent to ±57.6 degrees of phase error θ_1 for the loop to remove.

- Ramp of Error

If a ramp of frequency error with slope Δk (rad/s per second) is to be corrected, Equation (35) becomes

$$\omega_{VCO}(s) = \frac{\Delta k\ (a_0 + a_1 s + s^2)}{s^2(s+\alpha)(s+\gamma)}\ , \tag{42}$$

which has the inverse Laplace transform

$$\frac{\omega_{VCO}(t)}{\Delta k} = \frac{0.129}{\beta_0} + 0.000316t - \frac{1.25}{\beta_0} e^{-0.9\beta_0 t} + \frac{1.11}{\beta_0} e^{-0.11\beta_0 t}\ , t>0\ . \tag{43}$$

Even for relatively large sweep slope errors (Δk of $\pm 5\%$ of the 1000 MHz in 10 μs for example) the residual constant error term in Equation (43) is small (about $\pm 0.001\%$ of the 1000 MHz sweep). The two combined exponential terms for the same Δk do not exceed $\pm 0.0057\%$ of the 1000 MHz sweep (the maximum occurs at $t = 3\ \beta_0$) and are less than $\pm 0.001\%$ after $t = 20\ \beta_0 = 0.16\ \mu s$. These values indicate the systems can tolerate main sweep slope errors as large as about $\pm 5\%$.

The term of Equation (43) that is linear in t is a cumulative error. For the worst case (t=T) the maximum error $\pm 3.16(10^{-4})\Delta kT$ is less than $\pm 0.001\%$ of the 1000 MHz sweep if $\Delta k < \pm 2\pi(3.16)(10^{7})$ T rad s per second. This is about $\pm 3.2\%$ of the worst-case (smallest) system sweep slope. When these results are combined with those of the preceding paragraph, we see that system sweep slope errors of about $\pm 3.2\%$ can be loop compensated for any of the sweep period from 10μs to 100 μs.

- Sinusoidal Error

Examination of the nonlinear frequency errors of a typical Gunn device VCO [1, Figure 5] shows them to be approximately sinusoidal with about one cycle of error during each sweep. By assuming a sinusoidal error $\Delta\omega\sin(\beta t)$, where $\Delta\omega$ is the peak error in angular frequency in the sweep and β is the angular frequency of the error, Equation (35) becomes

$$\omega_{VCO}(s) = \frac{\beta\Delta\omega\ (a_0+a_1\ s + s^2)}{(s^2+\beta^2)\ (\ s + \alpha\ )(\ s + \gamma)} \ . \tag{44}$$

The inverse Laplace transform of Equation (44) is known, and, in terms of our loop design, reduces to

$$\frac{\omega_{VCO}(t)}{\Delta\omega} \simeq R_1\ e^{-0.9\beta_0 t} + R_2\ e^{-0.1\beta_0 t} + R_3\ \sin\ (\beta t + \Psi)\ ,\ t>0, \tag{45}$$

where ψ is an unimportant phase angle to the present discussion and

$$R_1 \simeq \frac{-101.4\ \chi}{8141.0+\ \chi^2} \tag{46}$$

$$R_2 \simeq \frac{1.37\chi}{123.0 + \chi^2} \tag{47}$$

$$R_3 \simeq \left\{ \frac{(0.32 - \chi^2)^2 + 1.73\,\chi^2}{(8141.0 + \chi^2)(123.0 + \chi^2)} \right\}^{\frac{1}{2}} \tag{48}$$

$$\chi = 100\ \beta/\beta_0 \quad . \tag{49}$$

The worst case of these errors occurs for the fastest sweep where one cycle of error per sweep corresponds to $\chi=1$. In this case $R_1 \approx -0.0125$, $R_2 \approx 0.011$ and $R_3 \approx 0.0015$. R_3 is the residual peak error after loop correction. If this error is to be within $\pm 0.001\%$ of the sweep, then for one cycle of error per sweep, $\Delta\omega < 2\pi(10^{-3})B\ R_3 \approx 2\pi(6.67)10^6$, which shows that a sweep peak nonlinearity of 6.67 MHz or 0.67% of B can be allowed. Of course, larger initial sweep nonlinearities are possible but residual error will be larger than $\pm 0.001\%$ of B.

For distortions of several periods per sweep ($1<\chi$), Equations (46) through (48) all increase proportional to χ for $1<\chi \lesssim 10$. Thus, the residual errors tend to increase as well for a fixed $\Delta\omega$. However, the Fourier series expansion of an arbitrary nonlinearity $\omega_1(t)$ nearly always produces harmonics that decrease in amplitude at least as fast as $1/n$. This means that $\Delta\omega$ for higher harmonics is expected to decrease about as fast as R_1, R_2, and R_3 increase in magnitude. The final conclusion is that no one harmonic component of $\omega_1(t)$ is expected to produce residual errors larger than the fundamental for $\chi=1$.

When the sum of the two exponential terms in Equation (45) is considered, it is found that the largest magnitude of error for $\chi=1$ occurs when $t = 2.9\ \beta_0 = 0.046\mu s$. The maximum value of residual error in $\omega_{\text{error}}(t)$ due to these terms is $7.3(10^{-3})\Delta\omega$. For this error to be less than 0.001% of B we require $\Delta\omega < 2\pi(1.37)10^6$ or a maximum uncorrected sweep error of 1.37 MHz (0.137% of B). Such a requirement is not likely to be true; therefore, the transient terms of Equation (45) are the dominant terms in the system. Fortunately, these terms die out rapidly with time. Their sum becomes less than the sinusoidal term's residual error (for the same $\Delta\omega$) when $t > 20\ \beta_0 = 0.32\mu s$ and therefore occur over only 3.2% of the period of the fastest sweep and 0.32% of the slowest sweep period.

To gain some overall insight into the linearity capability of the system *Figure 10* has been constructed based on preceding analyses and assuming sweep initial frequency error of 1% of B, an error of 5% of B in the sweep's slope, a peak sinusoidal error of 1% of B, and the shortest

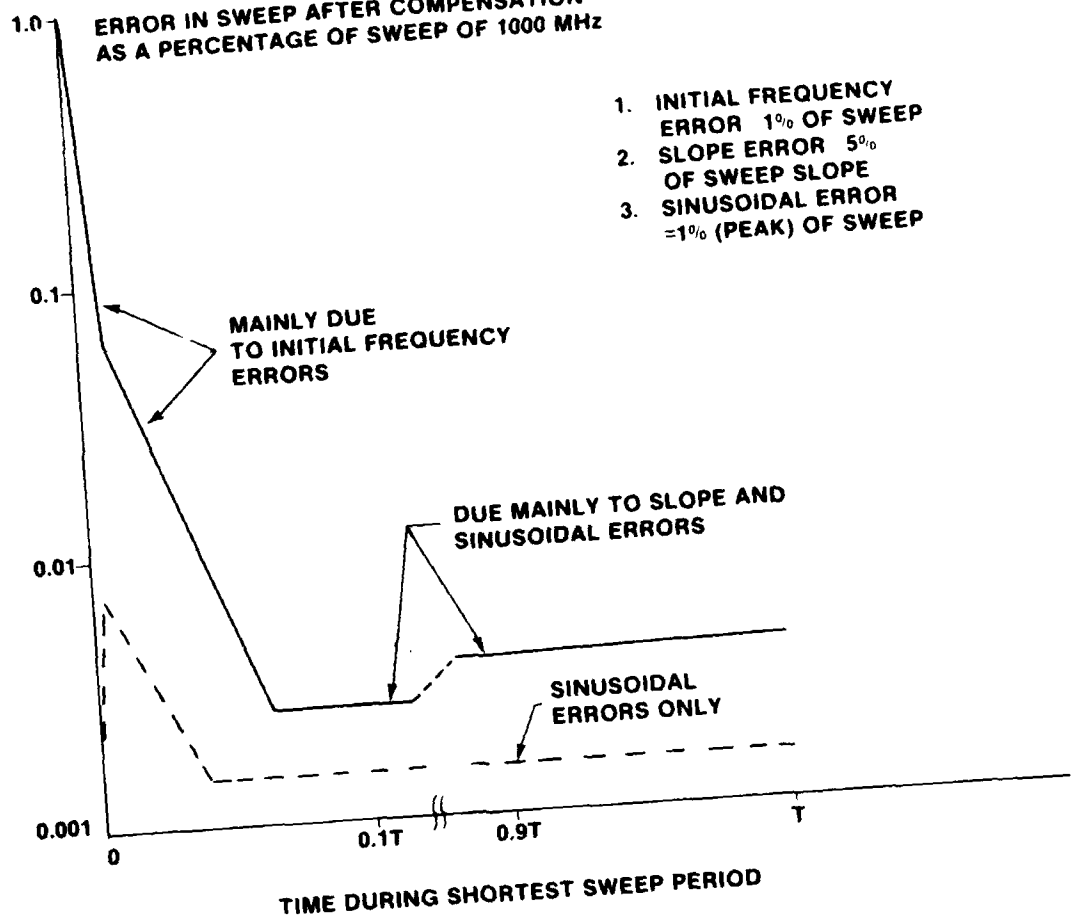

Figure 10. System linearity error.

sweep period of 10μs. At the start of the sweep linearity is only as good as initial frequency errors allow. These errors do not become negligible until about 6.4% of T after the sweep starts Thereafter, errors are due mainly to slope errors and sinusoidal errors. Ramp and sinusoidal errors are roughly equal in the time period shortly after 6.4% of T. Near the end of the sweep the sinusoidal error is about 40% of the total error. It is clear that initial frequency and slope errors are important. For comparison, the errors due to sinusoidal nonlinarity are shown dashed.

5. SUMMARY, DISCUSSION AND CONCLUSIONS.

At the present state-of-the-art, closed loop methods are capable of the best linearity in generating linear FM-CW sweeps. *Figure 1* illustrates about the best closed-loop system known at this time. Based on various practical design considerations, the system conceptually embodied in *Figure 1* is best implemented in the form of *Figure 4*. The overall loop behaves approximately as an automatic frequency control (AFC) loop.

This report has described various procedures necessary in the design of loops like that of *Figure 4*. Although numerical values have resulted from a desire to have a 1000 MHz sweep occur during a period T that is variable from 10μs to 100μs, the sweep being centered at 35 GHz, most of the procedures apply to any design.

The first design step is to choose the sweep period T (the minimum value if T is variable). Closed-loop bandwidth β_1 (rad/s) should then be chosen as large as possible to minimize the sweep time during which transient terms occur. Other bandwidth selection criteria were also given in the text. Present limits in the art for medium design difficulties appears to be about $\beta_1/2\pi$=10 MHz, which was chosen in the present system. At any rate, $\beta_1/2\pi \gtrsim 100/T$ should be chosen. With this choice the transient interval is about 6.4% of T.

The next design step is to select loop delay t_d according to $t_d \lesssim \pi/2\beta_1$. This choice will allow a loop having a phase margin of at least 39 degrees and gain margin of about 8 dB. The present system uses a delay t_d=16μs$<\pi/2\beta_1$=25ns because of practical considerations concerning the need for the system to operate over a decade range of T; its gain and phase margins are about 13dB and 56 degrees, respectively. These system values assume loop delay is small in relation to t_d. If delay is not small when the loop is constructed, it may be necessary to lower the loop bandwidth β_1 slightly to compensate for phase shifts introduced by the added delay.

Figure 9 illustrates a good choice of an open-loop transfer function where β_0 is an arbitrary unity-gain angular frequency and β_0=1/t_d. Because β_0 will approximately equal (but will be

slightly smaller than) β_1 one can design for any particular application once β_1 has been selected. Analysis of the closed-loop sweep linearization capability of the design leads to *Figure 10* which gives the percentage (of the sweep of B Hz) residual uncorrected sweep frequency errors as a function of time through the sweep period T. The data apply to a system with up to 1% (of B) initial frequency error (at the start of the sweep), up to 5% sweep slope error, and a sinusoidal open-loop VCO nonlinearity of 1% (of B). The results show a linearity error of about ±0.004% (of B) or less over 93.6% of the sweep period. Linearity error is as large as ±1% during the initial 6.4% of the sweep because of transients that occur while the loop is dynamically reducing open-loop errors to the steady-state closed-loop levels.

In summary, this report describes the design of a closed-loop system theoretically capable of improving the linearity of a "linear" FM-CW sweep from about ±1% linearity to about ±0.004% linearity. The reported effort is a continuation of an earlier study [1] to determine basic linearization concepts. The next logical extension of this work is the construction of a prototype system for evaluation. Efforts are being made in this direction at this time and it is hoped that results of evaluation will soon be available.

REFERENCES

1. P.Z. Peebles, Jr., "A Study of Sweep Linearity in Linear FM-CW Radar," *Technical Report* T-78-83, US Army Missile Research and Development Command, Redstone Arsenal, Alabama 35809.

2. W.J. Caputi, "Stabilized Linear FM Generator," *IEEE Transactions on Aerospace and Electronics Systems*, Volume AES-9, Number 5, September, 1973, pp. 670-678.

3. A. Blanchard, *Phase-Locked Loops, Application to Coherent Receiver Design*, John Wiley & Sons, New York, 1976.

4. Peyton Z. Peebles, Jr., *Communication System Principles*, Addison-Wesley, Reading, Massachusetts, 1976.

5. ITT Corporation, *Reference Data for Radio Engineers*, Fifth Edition, Howard W. Sams & Co., New York, 1970.

6. M. Abramowitz and I.A. Stegun (editors), *Handbook of Mathematical Functions with Formulas Graphs, and Mathematical Tables*, National Bureau of Standards Applied Mathematics Series, Volume AMS-55, June, 1964. (Available from US Government Printing Office, Washington, D.C. 20402).

DISTRIBUTION

	No. of Copies
Defense Documentation Center Cameron Station Alexandria, Virginia 22314	12
US Army Materiel Systems Analysis Activity ATTN: DRXSY-MP Aberdeen Proving Ground, Maryland 21005	1
IIT Research Institute ATTN: GACIAC 10 West 35th Street Chicago, Illinois 60616	1
DRSMI-LP, Mr. Voigt	1
DRSMI-TBD (R&D)	3
-TI (R&D) (Reference Copy)	1
-TI (R&D) (Record Set)	1
-T (R&D), Dr. Kobler	1
-TEG (R&D), Mr. Green	1
Dr. P.Z. Peebles, Jr. University of Tennessee Electrical Engineering Department Knoxville, Tennessee 37916	6

END

DATE
FILMED
1-82

DTIC